# Equilibrium and Diffusion of Methanol and Water in a Nafion 117 Membrane

**Craig M. Gates and John Newman**
Dept. of Chemical Engineering, University of California, Berkeley, CA 94720

*The uptake concentrations of methanol and water in a Nafion membrane are measured as a function of methanol mol fraction from a liquid methanol−water mixture. The results are fitted by a thermodynamically consistent equation, derived from an expression of the Gibbs energy. The uptake of pure methanol and pure water from the vapor phase is measured as a function of vapor pressure. A discontinuity, known in the literature as Schroeder's paradox, between membrane uptakes of pure methanol and pure water from the liquid and vapor phases is noted. Regions of unconditional instability are enveloped by spinodal loci for the ternary mixture in the membrane when equilibrated with liquid mixtures. The effective diffusion coefficient is measured at 60°C for diffusion from a vapor into a saturated Nafion membrane. The effective diffusion coefficients are found to be on the order of $10^{-11}$ $m^2/s$, which is comparable to other measurements made for diffusion of a vapor through the membrane.*

## Introduction

Fuel cells using proton-exchange membranes (PEM) show promise as a means for producing electrical power without shunt currents and at moderate temperatures suitable for portable power sources. In this article we consider the equilibrium and diffusion of methanol and water in Nafion 117 membrane used as the PEM for a direct methanol fuel cell (DMFC).

Nafion is a perfluorinated ion-exchange membrane that is fabricated by copolymerizing vinyl ether with Teflon, followed by hydrolyzing the sulfonyl fluoride group to the ionic sulfonate form. Nafion was originally produced for the manufacture of chlorine and caustic soda, and is known for its exceptional thermal and chemical stabilities and for its electrochemical properties. For these reasons, it is considered a candidate PEM for the DMFC.

Protons are produced at the anode by the direct oxidation of methanol in a DMFC. In order to design and optimize a fuel cell, it should be modeled with fundamental transport equations. These equations depend on transport properties that are functions of composition. The performance of the fuel cell will depend on the flow of protons from the anode, through the membrane, to the cathode. The transport properties that relate to this process are the membrane's ionic conductivity, the diffusion coefficients for those species, and electroosmotic coefficients for the solutes. Zawodzinski et al. (1993a) note the dependence of conductivity and diffusion coefficients on solute concentration in Nafion.

The objectives of this work are to measure the uptake concentration of methanol and water and their diffusion in a Nafion® membrane, and to calculate the activities and concentrations of methanol and water in the membrane phase with a thermodynamically consistent equation. The equilibrium experiments are limited to mixed-solvent uptake in the liquid phase and single-solvent uptake in the vapor phase; the measurement of the diffusion coefficient is limited to the combined diffusion coefficient calculated from the restricted diffusion method as given by Harned and French (1945).

## Equilibrium of Methanol and Water in Nafion

To determine the membrane-phase composition as a function of liquid-phase composition, it is necessary to calculate the activities of methanol and water in the membrane phase and compare them to the activities in the liquid phase. The activity for each component in the liquid phase can be estimated from vapor−liquid equilibria listed by Hirata et al. (1975). Liquid-phase activities and experimental binary solute−membrane and ternary solute−solute−membrane data should allow us to estimate the membrane composition of each solute.

---

Correspondence concerning this article should be addressed to J. S. Newman.
Current address of C. M. Gates: Hewlett Packard Company, 1000 NE Circle Blvd., Corvallis, OR 97330.

The chemical potential $\mu_i$ of a liquid is defined by the partial molar Gibbs energy of species $i$:

$$\mu_i \equiv \left(\frac{\partial G}{\partial n_i}\right)_{\substack{T,P,n_j\\ i\neq j}} = \mu_i^{o} + RT\ln a_i = \mu_i^{o} + RT\ln x_i\gamma_i, \quad (1)$$

where $\mu_i^{o}$ defines the standard state of the liquid and is a function of temperature and pressure, $\gamma_i$ is the activity coefficient and accounts for deviations from ideality, $x_i$ is the mol fraction, $a_i$ is the activity of species $i$, $T$ is the absolute temperature, and $R$ is the gas constant. For systems at thermal and mechanical rest, the chemical potential $\mu_i$ is constant across a phase boundary for each component, which allows us to write a phase-equilibrium equation:

$$\mu_i^{*} + RT\ln\phi_i y_i p = \mu_i^{o} + RT\ln\gamma_i x_i, \quad (2)$$

where the superscript * denotes the vapor-phase reference state, $\phi_i$ is the fugacity coefficient of $i$ in the vapor phase, $y_i$ is the mol fraction of $i$ in the vapor phase, and $p$ is the total pressure. The vapor-phase fugacity coefficient $\phi_i$ can be calculated by integrating the virial equation of state over the range of pressure from 0 to $p$. The activity of the liquid can be calculated from the experimental composition, temperature, and pressure and the calculated $\phi_i$.

From the perspective of designing a fuel cell, it is desirable to predict solute uptake. This can be done by knowing $a_i$ as a function of composition, temperature, and pressure. When dealing with a multicomponent system, however, it is useful to start with an expression of the total Gibbs function, $G$, to ensure that no inconsistencies are involved in the thermodynamic development. For this work, we start with a Margules form to account for the nonidealities:

$$G = \sum_i n_i\mu_i^{o} + RT\sum_i n_i\ln x_i + \frac{1}{2}\sum_i\sum_j A_{ij}n_ix_j + \frac{1}{3}\sum_i\sum_j\sum_k B_{ijk}n_ix_jx_k + \ldots, \quad (3)$$

where $n_i$ is the number of moles, and the $A$'s and $B$'s are fitting parameters.

Equation 3 defines the total Gibbs function in terms of mol fractions. In polymer systems the equivalent molar volume $(EW/\rho)$ of the polymer may be much larger than the molar volume of the solutes; consequently, the mol fractions of the solute may approach unity. With this in mind, we redefine Eq. 3 in terms of $z_i$

$$G = \sum_i n_i\mu_i^{\bullet} + RT\sum_i n_i\ln z_i + \frac{1}{2}\sum_i\sum_j A_{ij}q_in_iz_j + \frac{1}{3}\sum_i\sum_j\sum_k B_{ijk}q_in_iz_jz_k, \quad (4)$$

where we define $z_i$ as

$$z_i \equiv \frac{n_iq_i}{\sum_j n_jq_j},$$

**Table 1. Parameters for Eq. 4 for Liquid Methanol and Water in Equilibrium with Nafion at 60°C**

| Parameter | Value |
|---|---|
| $A_{12}/RT$ | 0.036 |
| $B_{112}RT$ | −0.009 |
| $A_{13}/RT$ | 0.047 |
| $B_{113}/RT$ | 0.01 |
| $A_{23}/RT$ | 0.0 |
| $B_{223}/RT$ | 0.013 |
| $B_{123}/RT$ | 0.016 |
| $q_1$ (cm$^3$/mol) | 17.7 |
| $q_2$ (cm$^3$/mol) | 40.77 |
| $q_3$ (cm$^3$/mol) | 597.8 |

and the $q_i$ are independent of molar composition, but may depend on $T$ and $p$. The $q_i$ are commonly taken to be the molar volumes of the pure components, but molecular weights $M_i$ cold be used instead. In this treatment, molar volumes listed in Table 1 are used. Equation 4 is similar to Wohl's form, but here we use $z_i$ instead of $x_i$ in the logarithmic term. Also, $\mu_i^{\bullet}$ is a secondary-reference state quantity that could be different from $\mu_i^{o}$, which refers to pure liquid. Newman (1985) notes that the distinctions made with the indices allow us to add restrictions to the fitting parameters. If the first term in Eq. 4 is regarded as the secondary-reference-state contribution from the pure components, then for a pure component, the remaining terms must equal zero, requiring that $A_{ii}$ and $B_{iii}$ be zero. Inspection of Eq. 4 shows that $A_{ij}$ can be set equal to $A_{ji}$, since $n_iz_j = n_jz_i$. Similar reasoning allows us to make restrictions on the $B_{ijk}$. Since the volume fractions $z_i$ are not independent in a mixture, we can also write $B_{ijj} = -B_{iij}$.

By differentiating Eq. 4 with respect to $n_\alpha$ according to Eq. 1, we obtain a general expression for the chemical potential:

$$\mu_\alpha = \mu_\alpha^{\bullet} + RT\ln z_\alpha + RT\left[1 - q_\alpha\frac{\Sigma_j n_j}{\Sigma_k n_kq_k}\right] + \frac{1}{2}q_\alpha\left[\sum_j A_{\alpha j}z_j + \sum_i A_{i\alpha}z_i + \sum_i\sum_j A_{ij}z_iz_j\right] + \frac{1}{3}q_\alpha\left[\sum_i\sum_j B_{ij\alpha}z_iz_j + \sum_i\sum_k \times B_{i\alpha k}z_iz_k + \sum_j\sum_k B_{\alpha ik}z_jz_k - 2\sum_i\sum_j\sum_k B_{ijk}z_iz_jz_k\right]. \quad (5)$$

If we modify the definition of $\gamma_i$ from Eq. 1 to $a_i = z_i\gamma_i$, then the activity coefficient $\gamma_i$ is given by

$$RT\ln\gamma_\alpha = \mu_\alpha^{\bullet} - \mu_\alpha^{o} + RT\left[\frac{\Sigma_j n_j(q_j - q_\alpha)}{\Sigma_k n_kq_k}\right] + \frac{1}{2}q_\alpha\left[\sum_j A_{\alpha j}z_j + \sum_i A_{i\alpha}z_i + \sum_i\sum_j A_{ij}z_iz_j\right] + \frac{1}{3}q_\alpha\left[\sum_i\sum_j B_{ij\alpha}z_iz_j + \sum_i\sum_k B_{i\alpha k}z_iz_k + \sum_j\sum_k B_{\alpha ik}z_jz_k - 2\sum_i\sum_j\sum_k B_{ijk}z_iz_jz_k\right]. \quad (6)$$

The use of $z_i$ instead of $x_i$ allows us to deal better with a polymer system. Specifically, the equation for liquid−mem-

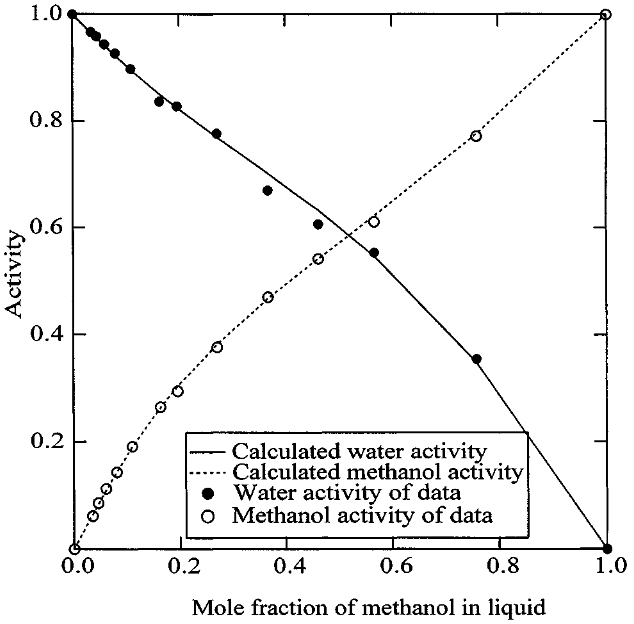

**Figure 1. Vapor–liquid equilibrium activity fit at 60°C, with the activity coefficient of Eq. 6.**

The data are thermodynamically consistent by virtue of their agreement to a model with a thermodynamic basis. The data come from Hirata et al. (1975). The values of the parameters are listed in Table 1.

brane equilibrium becomes:

$$z_i^o \gamma_i^o = z_i^\bullet \gamma_i^\bullet, \tag{7}$$

where o denotes the liquid phase and $\bullet$ denotes the membrane phase, and we have set $\mu_i^\bullet = \mu_i^o$. Equation 6 allows us to calculate thermodynamically consistent activities for each of the species present for a given set of $A$'s and $B$'s.

The general form of the Gibbs function has the feature that it should reduce to describe a binary system. Thus, some of the binary parameters ($A$'s and $B$'s) can be found by fitting binary data. For this work, we fitted Eq. 6 to binary vapor–liquid equilibrium data from the literature for methanol and water at 60°C. Figure 1 shows the fit we obtained for vapor–liquid–equilibria, thereby setting the values of $A_{12}$ and $B_{112}$. The composition of the liquid phase allows us to calculate the liquid-phase activity in Eq. 7. By measuring the uptake composition, we can then fit our ternary data to Eq. 7.

Zawodzinski et al. (1993a,b), Nandon et al. (1992), and Hinatsu et al. (1994) studied the uptake of water in Nafion in the literature; however, there is very little on the uptake of methanol. None of this work is described on a thermodynamic basis. Nandan et al. (1992) give the uptake of liquid water and methanol at 25°C and a datum for uptake from an equimolar methanol–water liquid mixture at the same temperature. Skou et al. (1997) reports the uptake of methanol and water from liquid mixtures at ambient conditions. The uptake was found to equal 22 moles of solute per sulfonic acid site when the membrane was equilibrated with pure methanol. The experimental procedure was similar to the method we present in this work; however, they heated their membrane only to 70°C for 30 min in a vacuum oven and their compositional analysis was done by nuclear magnetic resonance (NMR). To our knowledge, we are the first to fit data from the uptake of liquid methanol–water mixtures in Nafion to an equation that has a thermodynamic basis.

Other polymer membrane systems have been treated more completely. Heintz and Stephan (1994) use the UNIQUAC model to fit uptake of water and methanol in a poly(vinyl alcohol) membrane. In that work, they note a discontinuity in uptake from vapor and liquid phases; this is known in the literature as Schroeder's paradox (Schroeder, 1903).

## Diffusion Coefficients from Uptake Measurements

The diffusion of two solutes in a membrane is regarded as a multicomponent diffusion problem, since the flux of one species is coupled to the flux of the others present. This coupling prevents the straightforward calculation of the binary interaction parameters. However, an effective diffusion coefficient of the solutes can be measured.

Harned and French (1945) developed a method to measure the restricted diffusion of a solute in a finite column of solvent. By measuring the uptake with time, diffusion coefficients at different hydration states can be determined. Fuller (1992), Yeo and Eisenberg (1977), and Zelsmann and Pineri (1990) studied the diffusion of water or methanol in Nafion. Here, the restricted diffusion method is applied to uptake of methanol and water in Nafion. This method requires measuring the decay of a concentration gradient between two points in the column.

Solute uptake can be described by Fick's second law if an effective diffusion coefficient is considered:

$$\begin{gathered} \frac{\partial c_m}{\partial t} = D_m \nabla^2 c_m \\ c_m = \text{constant at } x = 0 \text{ and } x = l \\ \nabla c_m = 0 \quad \text{at } x = l/2, \end{gathered} \tag{8}$$

where the subscript denotes the measured values. Here the swelling of the membrane with solute is not accounted for. The boundary conditions given here correspond to the problem of uptake by a slab of thickness $l$, as indicated below.

Chapman (1967) gives the solution to Eq. 8 for a slab geometry as an expansion of a Fourier series

$$c_m(x,t) = c_0 + \sum_{n=1}^{\infty} A_n \exp^{-((n^2\pi^2 D_m/l^2)t)} \cos\left(\frac{n\pi x}{l}\right). \tag{9}$$

At long times, the series converges, and a plot of ln $\Delta c_m$ vs. $t$ gives a slope equal to $D_m\pi^2/l^2$.

The diffusion coefficient can be determined by measuring the mass of the membrane vs. time. Here, the natural log of the difference between membrane mass and the final membrane mass can be plotted vs. time to determine $D_m$, since the slope is again equal to $D_m\pi^2/l^2$.

## Experimental Design and Procedure

The Nafion membranes used in this work were pretreated using a procedure similar to the methods presented by Nandon et al. (1992), Hinatsu et al. (1994), and Zawodzinski et al. (1991). Pretreatment is necessary to erase the polymer's history, which affects the morphology of the ionic clusters, and hence its ability to absorb solutes. The process includes boiling the membrane for one hour in each of the following: a 3% $H_2O_2$ solution, deionized water, 0.5-M solution of $H_2SO_4$, followed by deionized water. Zawodzinski et al. (1991) and Hinatsu et al. (1994) have noted a discontinuity in Nafion's uptake of water from the liquid and vapor phases. In this work, we collected uptake data from both types of experiments. The diffusion experiments were done via vapor-phase uptake.

### *Liquid-phase experiments*

Liquid-phase experiments were performed by soaking a sample of pretreated membrane in a liquid solution of known composition until it became equilibrated with the liquid solution. The time required for equilibration should be on the order of an hour, that is, $l^2/D$, where $D$ is the diffusion coefficient and $l$ is the membrane thickness; however, the samples were usually allowed to equilibrate for 1 to 2 days. Samples were prepared at 20 and 60°C at atmospheric pressure. When the uptake composition from the membrane was analyzed, a sample of the liquid solution was also analyzed.

A diagram of the solvent-recovery apparatus is given in Figure 2. The system consists of a flask fitted with a wide mouthed opening, which allows easy access to insert or remove the membrane. The flask is connected to a vacuum pump with an in-line recovery container held in a cold trap at 77 K. The entire system is kept in a Plexiglas box to minimize th effects of air drafts on solvent evaporation or absorption during the transfer to or removal from the flask.

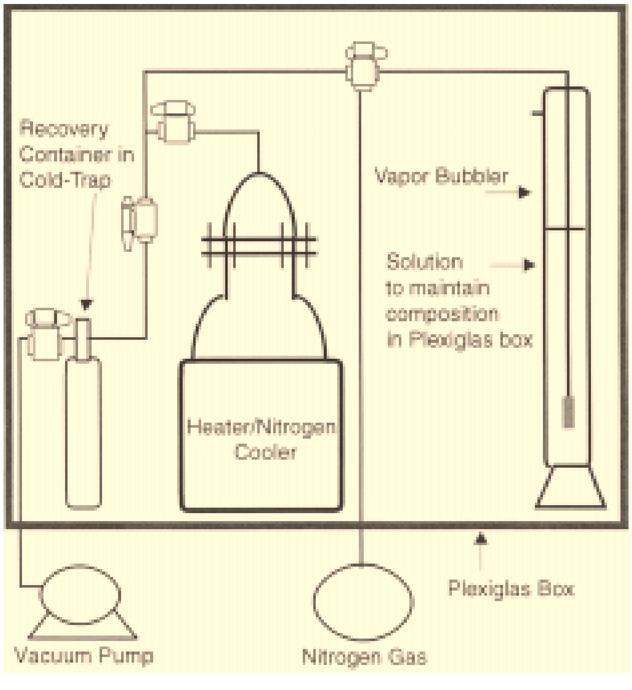

**Figure 2. Solvent-recovery apparatus for liquid-phase experiments.**

After the membrane was equilibrated with the liquid mixture, it was quickly surface dried using a lint-free tissue. It was then placed in the widemouthed flask and heated under vacuum to separate the solutes from the Nafion.

After the membrane was allowed to equilibrate with the liquid solution, it was weighed and placed in the flask shown in Figure 2. The flask was then heated to 105°C and held at that temperature for 1 h. The solutes evaporate from the membrane and condense in the recovery container, which remained connected to the vacuum system. The composition of the solutes is determined by analyzing the solute mixture by Karl-Fischer titration.

### *Vapor-phase experiments*

Vapor-phase experiments were performed using a gravimetric sorption apparatus. This method requires suspending a sample of pretreated membrane in a vapor of the solute. The sample is suspended on a calibrated quartz spring (obtained from Ruska Instruments Corp., Houston, TX); its mass is determined by measuring the spring deflection using a cathetometer. A diagram of the gravimetric sorption apparatus used for this work is given in Figure 3.

The system is placed in an air bath maintained at 60°C. The glass chamber is constructed of two pieces of glass that form a tall enclosed vapor space to allow extension of the spring when its load is increased. The spring is calibrated at the system temperature with weights that span the spring's load capacity. Springs are available with different capacities and sensitivities. The height inside the glass chamber is 0.25 m. The sensitivities of the springs used during this work var-

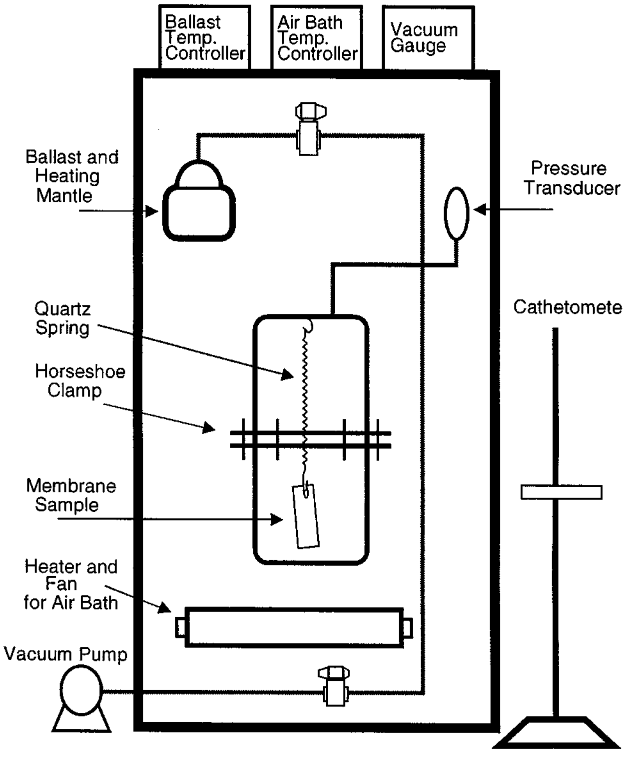

**Figure 3. Gravimetric sorption apparatus used for vapor-phase uptake experiments.**

A pretreated membrane was placed on the hook in the vacuum chamber. After evacuating the system, the solute was vaporized by opening the valve to the ballast. The spring deflection was measured at different vapor pressures after equilibrium had been attained.

ied around $1 \times 10^{-3}$ kg/m. The precision of the cathetometer is $5 \times 10^{-5}$ m. This gives a mass measurement with the precision of $5 \times 10^{-8}$kg. The system should be evacuated to $<100$ Pa, and held overnight without gaining more than 100 Pa. The vacuum gauge used was a digital Varian WV100 model with a transducer containing both a low- and mid-vacuum sensor. The thermocouple was calibrated by taking the average temperature on four sides of the spring chamber.

A pretreated membrane was soaked in a liquid solution before being cut to a weight no greater than the maximum weight limit of the spring. This ensures that the mass of solute can be measured accurately without breaking the spring.

The solute was held in a flask that was thermally insulated from the spring chamber housing. By controlling the temperature of the flask separately from the spring chamber, the vapor's partial pressure, and hence its activity, could be varied. The flask was filled with solute, placed in a heating mantle, and connected to the spring chamber with stainless-steel tubing. The temperature of the flask was controlled to produce a vapor of the desired pressure. Spring deflection was measured at each pressure after allowing a couple of hours to ensure that the membrane was equilibrated with the vapor. A calibration curve was used to calculate the membrane's mass from the spring's deflection. After the last measurement, the membrane was heated to 105°C under vacuum for 1 h and its mass recorded.

### *Diffusion experiments*

Diffusion-coefficient experiments were performed using a Cahn 2000 microbalance. The electrical torque sensor was housed in an aluminum box equipped with a convective fan, heating element, thermocouple, and tube supplying vapor from the solute. The heater was maintained at 60°C with a temperature controller attached to the thermocouple. The vapor was supplied by bubbling nitrogen through a series of two bubblers immersed in a bath maintained at 50°C. An output voltage proportional to the mass of the sample was generated by a multimeter. The output voltage from the torque sensor was converted to a value for total mass (kg) and recorded to a file. A diagram of the equipment layout is given in Figure 4.

A pretreated, soaked membrane was placed on the hook connected to the torque sensor, and the valve opened to allow nitrogen to flow through the heated solutions in the bubblers. The valve was opened enough to allow approximately one volume (the volume of the sensor enclosure) change every 5 min. At the end of the experiment, the membrane was dried and its mass recorded.

## Results and Discussion of Equilibrium Uptake

The equilibrium results show two interesting qualitative features. The first is a discontinuity in uptake of each solute between vapor–membrane equilibrium and liquid–membrane equilibrium. Zawodzinski et al. (1991) point out this phenomenon for the water–membrane system. The second is an increase in the solubility of methanol and water when both solutes are present, as depicted in Figure 5. This increase has not been noted in the literature for a methanol, water, and Nafion system, but it was discussed for other systems by Skou et al. (1997) and Hauser et al. (1989).

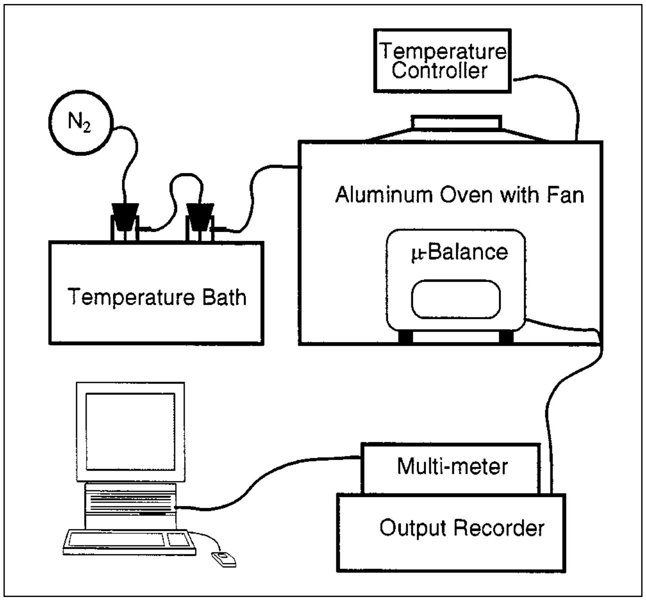

**Figure 4. Equipment used for diffusion experiments.**

The membrane was suspended in a microbalance enclosed in an oven held at 60°C. Nitrogen was bubbled through two flasks of liquid mixture with a known composition. The vapor stream was connected to the oven, where it was absorbed by the membrane.

The Gibbs function in Eq. 4 and the derived activity coefficients in Eq. 6 form the basis for treating the equilibrium data. Vapor–liquid data from Hirata et al. (1975) were fitted on this basis (Figure 1) and provide the source of information on the activities of methanol and water as well as values for

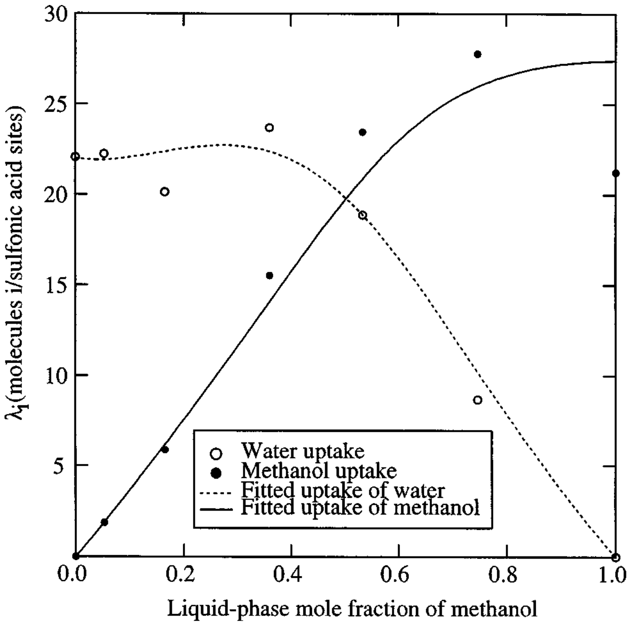

**Figure 5. Uptake of methanol and water at 60°C.**

Solute uptake from the liquid phase as a function of liquid-phase composition; $\lambda$ is the number of solute molecules per sulfonic acid site. The fitted curves were calculated using the parameters in Table 1.

**Table 2. Data from the Measurements of Liquid-Phase Samples at 60°C**

| Liq. Mol Fraction of $CH_3OH$ | Total Mass ($\times 10^{-6}$ kg) | Recovered Mass ($\times 10^{-6}$ kg) | Dry Memb. ($\times 10^{-6}$kg) | $CH_3OH$ Mol Fraction of Recovered Mass | Calc. Activity $CH_3OH$ | Calc. Activity $H_2O$ |
|---|---|---|---|---|---|---|
| 0 | 694 | | 510 | 0 | 0 | 1 |
| 0.055 | 1,396 | 374 | 985 | 0.077 | 0.101 | 0.946 |
| 0.164 | 1,364 | 363 | 909 | 0.226 | 0.266 | 0.850 |
| 0.358 | 1,464 | 604 | 796 | 0.396 | 0.460 | 0.709 |
| 0.540 | 1,531 | 656 | 769 | 0.555 | 0.602 | 0.569 |
| 0.749 | 1,020 | 362 | 523 | 0.762 | 0.769 | 0.359 |
| 1 | 330 | | 204 | 1 | 1 | 0 |

the binary coefficients $A_{12}$ and $B_{112}$. Schroeder's paradox prevents us from obtaining the other binary parameters ($A_{13}$, $A_{23}$, $B_{113}$, and $B_{223}$) from the binary membrane–methanol and membrane–water systems because vapor must be used.

### *Liquid–membrane equilibrium*

The data for the uptake of methanol and water from liquid solutions at 60°C are given in Table 2 and plotted in Figure 5. The data can also be represented on the triangular diagram in Figure 6, where they provide the tie lines between the liquid (methanol, water) phase and the membrane phase. The end points of the experimental tie lines are open circles and filled circles. The remaining parameters ($A_{13}$, $A_{23}$, $B_{113}$, $B_{223}$, and $B_{123}$) are adjusted to match as closely as possible the experimental tie lines, as discussed below. The calculated phase boundaries are plotted as dashed lines. The binary membrane–methanol point is not well fit. The calculated results are also transcribed onto Figure 5, showing a direct comparison of experimental and thermodynamically consistently calculated compositions.

Parameters $A_{12}$ and $B_{112}$ were determined by fitting the literature data in Figure 1 for methanol–water vapor–liquid equilibrium at 60°C. Parameters $A_{13}$ and $B_{113}$ together determine the water–membrane binary equilibrium; if $B_{113}$ is changed, $A_{13}$ can be changed to compensate and yield the same binary point. This gives a degree of freedom in fitting the ternary data. Similarly, $A_{23}$ and $B_{223}$ determine the methanol–membrane binary equilibrium, leaving a degree of freedom. Finally, the parameter $B_{123}$ affects only the ternary data. This means that $B_{113}$, $B_{223}$, and $B_{123}$ can be adjusted simultaneously to fit the ternary two-phase data, with $A_{13}$ and $A_{23}$ constrained so that the binary membrane points are preserved. The parameters used to fit the data in Table 2 are listed in Table 1.

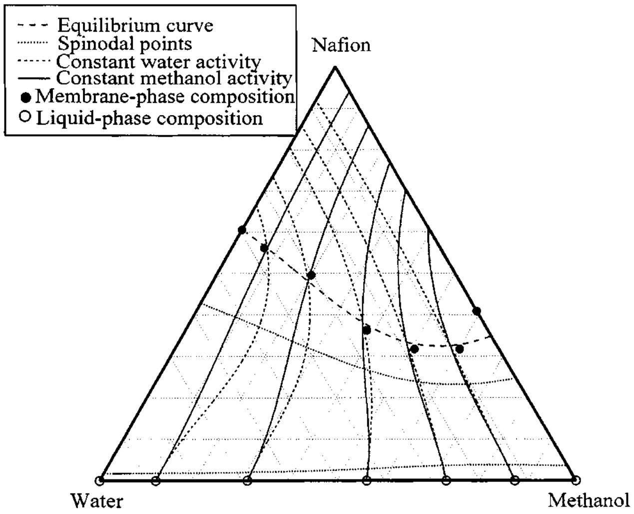

**Figure 6. Ternary diagram (in volume fraction, $z_i$) for methanol–water–Nafion equilibrium at 60°C.**

The binary water–membrane point is well fit on Figures 5 and 6, but the fit of the binary methanol–membrane point needed to be compromised so that the ternary data could be approximated better. The evaporation of methanol affected our measurements, leading the experimental value of uptake to fall below the fitted value.

Figure 6 also shows lines of constant activity (dotted for water and solid for methanol) that correspond to the compositions of the liquid-phase solutions with which the membranes were equilibrated at 60°C. The constant-activity lines start on the binary water–methanol liquid-phase boundary and enter into the membrane region, terminating on the binary methanol–Nafion line or on the binary water–Nafion line. The points on the methanol–water line correspond to the compositions of the liquid methanol–water mixtures.

The equilibrium concentrations are predicted where both of the constant-activity lines that originate from the liquid solution intersect in the membrane region of the graph. The loci of such intersection points are drawn on Figure 6 as two equilibrium curves. The departure of the experimental points from the intersection represents the deviation of the fit, due to a combination of experimental error and a limited fitting function. The upper equilibrium line corresponds to ternary equilibrium when the liquid solutes are absorbed by the membrane. The lower equilibrium curve runs along the methanol–water base line and shows the equilibrium we should expect if the membrane were soluble in the liquid phase. Also shown are two envelopes of spinodal points that define a region of unconditional instability. Spinodals are defined as points where the activities of two components go through extrema when the activity of the third component is held constant. Table 3 shows the values of the liquid- and membrane-phase volume fractions, activities of each component for each datum, and the coordinates for the spinodal points.

By plotting the activity of the membrane vs. the activity of one solute along a line of constant activity for the other so-

**Table 3. Liquid- and Membrane-Phase Equilibrium Compositions and Spinodal Points at 60°C**

| $x$CH$_3$OH, Liquid | $z$CH$_3$OH, Liquid | $z$H$_2$O (1) Memb. Data | $z$ CH$_3$OH (2) Memb. Data | Activity H$_2$O($a1$) | Activity CH$_3$OH($a2$) | Spinodal (constant $a1$) ($z1/z2$) | Spinodal (constant $a2$) ($z1/z2$) |
|---|---|---|---|---|---|---|---|
| 0 | 0 | 0.395 | 0 | 1 | 0 | 0.561/0.0<br>0.981/0.0 | — |
| 0.055 | 0.118 | 0.369 | 0.069 | 0.946 | 0.101 | 0.477/0.152<br>0.865/0.117 | 0.515/0.090<br>0.864/0.118 |
| 0.164 | 0.311 | 0.304 | 0.200 | 0.850 | 0.266 | 0.401/0.278<br>0.670/0.309 | 0.424/0.239<br>0.670/0.310 |
| 0.358 | 0.562 | 0.254 | 0.384 | 0.709 | 0.460 | 0.296/0.439<br>0.421/0.551 | 0.306/0.424<br>0.412/0.552 |
| 0.540 | 0.730 | 0.177 | 0.507 | 0.569 | 0.602 | 0.206/0.556<br>0.260/0.704 | 0.211/0.550<br>0.259/0.705 |
| 0.749 | 0.873 | 0.081 | 0.601 | 0.359 | 0.769 | 0.101/0.661<br>0.124/0.838 | 0.110/0.657<br>0.123/0.839 |
| 1 | 1 | 0 | 0.591 | 0 | 1 | — | 0.0/0.750<br>0.0/0.965 |

lute (Figure 7), two features are illustrated: the region of instability between spinodal points and the intersection where the activities of solutes in the membrane phase are equal to those in the liquid phase. These intersections predict the equilibrium points in a three-component system, as the intersecting lines correspond to the compositions of the two phases.

In the liquid-phase experiments presented in this work, the solutes must be separated from the membrane and analyzed for water content. The measurements for this work include the total mass of the Nafion–water–methanol system; the mass of the dried membrane, found after the solutes are removed; and the composition of water in the recovered uptake fraction, which is determined by a Karl-Fischer titration. The difference in total uptake and mass of the membrane is the mass of the uptake fraction. Also, the mass of the recovered uptake fraction is measured, and compared to the total uptake in Table 2. Presumably, the composition of the recovered fraction is close to that absorbed by the membrane.

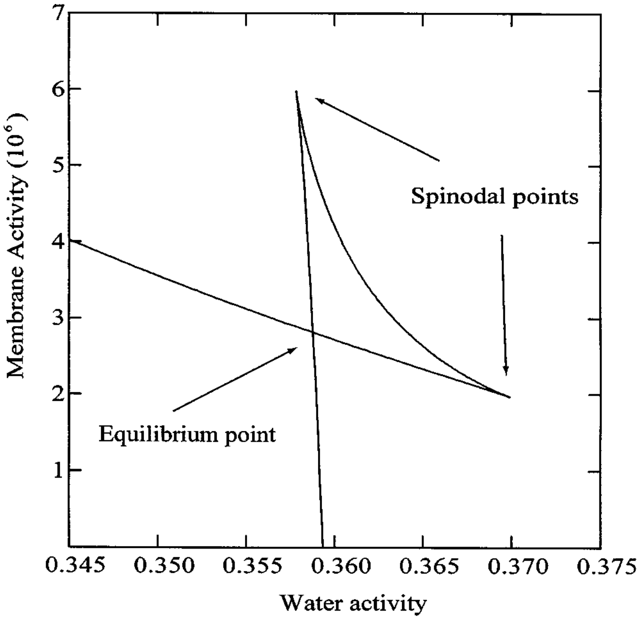

**Figure 7. Spinodal points found for methanol–water–Nafion equilibrium at 60°C.**

At constant methanol activity of 0.769, corresponding to a liquid composition of $x = 0.749$, this graph shows that the activities of water and membrane at two different compositions are equal. These compositions are the liquid- and membrane-phase equilibrium points.

After the data were collected from the uptake experiments for pure water or methanol equilibrium, the membranes were pretreated again to see if the measurements were repeatable. In both cases, the results were within $\lambda = \pm 1$.

There are two sources of experimental error in these experiments: those errors stemming from the assumption that all of the solutes are recovered, and analytical errors from measuring compositions and masses. The former can be addressed by considering the surface drying and transferring step to the recovery system, and the separation process. After the membrane had been equilibrated with the liquid solution, it was surface dried with a lint-free tissue in an environment presumably saturated with vapor from the liquid solution. The purpose of surface drying is to remove liquid droplets not absorbed in the membrane. This step introduces uncertainty in both the total mass measurement and the subsequent compositional analysis. If the surface is not completely dried, the measured mass will be too high, and the composition will be influenced toward that of the liquid phase. On the other hand, evaporation from the membrane during, or after, drying would reduce the recovery and make it leaner in methanol. This is expected because the membrane temperature is near the boiling point of methanol at atmospheric pressure. Another source for the recovery discrepancy is due to the separation process. Methanol and water are separated from the membrane using a thermal gradient at low pressures. Here the recovery vessel was held at the temperature of boiling nitrogen, 77 K, while the membrane was gradually heated to and held at 105°C for about 1 h. In the design of the separation system it was assumed that the saturation pressure of each solute was so low at 77 K that substantially all of the solutes would be drawn from the warm membrane and condensed in the recovery vessel. However, poor heat transfer could account for some losses to the vacuum system. The exact times were not watched closely enough to discern any time dependence on uptake recovery. In retrospect, it would have been better to shut the valve to the vacuum line.

Errors arising from the precision of the mass measurements, $\pm 1 \times 10^{-6}$ kg, yield a negligible error. The remaining source for error is derived from the accuracy of the Karl-Fischer titration for the compositional analysis of water. The Karl-Fischer factor was found by titrating a known amount of water. Any errors in either the volume of titrant or the mass of the sample would correspond to an error in the water composition of the sample. Repeatability measurements were made for membrane samples absorbing from each solute from the liquid phase. Uptake from both liquid water and methanol was measured within $\lambda = \pm 1$.

### *Vapor-phase equilibrium*

Zawodzinski et al. (1991) measured the uptake of water vapor in Nafion at 30°C as a function of water activity. They used the isopiestic sorption method. Their result for unit activity was $\lambda = 14$. Hinatsu et al. (1994) performed similar experiments at 80°C using the gravimetric sorption method with a result of $\lambda = 9.2$. Our result at 60°C is $\lambda = 8.3$. We compare these isotherms in Figure 8.

Figure 8 shows three isotherms for water-vapor uptake as a function of partial pressure. The figure shows that the uptake increases along an isotherm as the vapor activity approaches unity at the end points. An error in the temperature of the membrane and vapor would result in an error in the measured uptake, and the end point—the uptake from the vapor at unit activity—would not have been found. Vapor pressure has an exponential dependence on temperature, and small errors in temperature propagate as larger errors in pressure measurements. This would result in inaccurate calculation of the vapor-phase activity.

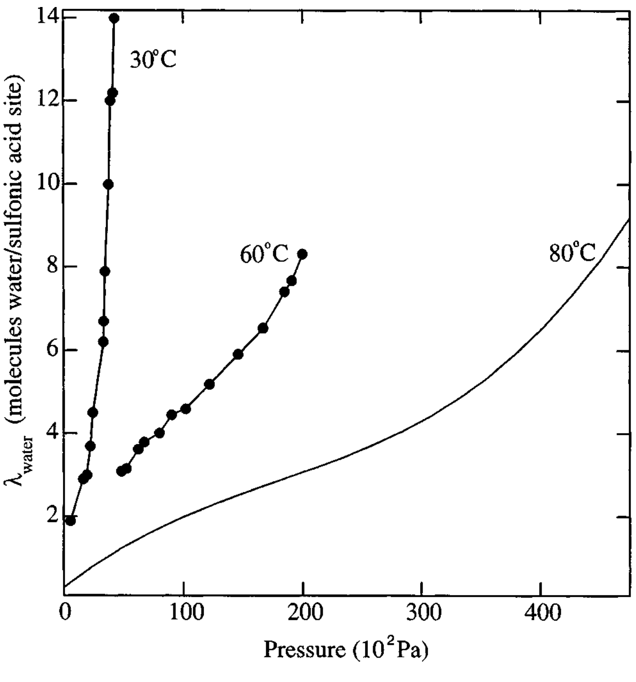

**Figure 8. Water-vapor uptake isotherms at 30°C (Zawodzinski et al., 1991), 60°C (this work), and 80°C (Hinatsu et al., 1994).**

The data for 30°C were collected using an isopiestic method; the data at 60°C and 80°C were collected using a gravimetric sorption method. The data of Hinatsu et al. (1994) are expressed using their least-squares fit.

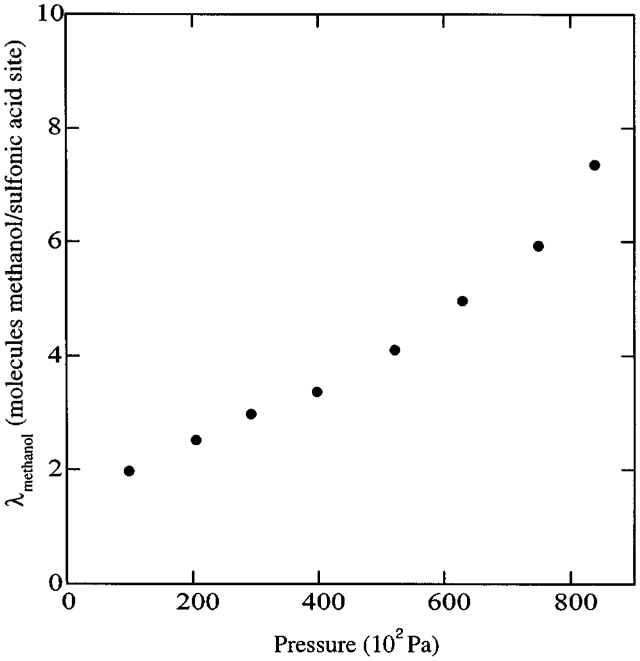

**Figure 9. Methanol–vapor uptake at 60°C; these data were obtained using a gravimetric sorption apparatus.**

We were unable to find Nafion uptake of methanol from the vapor phase in the literature. However, we observed a discontinuity of uptake from vapor and liquid phases, similar to that found for water. The uptake of methanol is plotted vs. pressure in Figure 9; the value at unit activity is $\lambda = 7.35$. Our measured uptake from liquid methanol was $\lambda = 21.5$; however, this may be a low value because methanol has a high partial pressure at 60°C and either some evaporation took place during the membrane drying process or the heat transfer was not sufficiently great to allow the vapor to reach 77 K. The value calculated from the data fit (Figure 5 or 6) is $\lambda = 27.5$. Skou et al. (1997) give a value of $\lambda \approx 22$. Repeatability measurements from the vapor phase tended to be very close to the reported values, $\lambda = \pm 0.1$. Results from the vapor-phase uptake experiments were more reproducible than those from the liquid phase due to the lack of handling required to measure the mass change of the membrane.

## Results and Discussion of Diffusion-Coefficient Measurement

We measured the time dependence of uptake from the vapor phase at 60°C in three experiments. The first was a water-saturated membrane exposed to methanol vapor (Figure 10). The second experiment, shown in Figure 11, was the same membrane, presumably saturated with methanol, exposed to water vapor. The final experiment was the uptake of a vapor in equilibrium with an equimolar liquid mixture of water and methanol into a water-saturated membrane (Figure 12). Here the final mass $m_f$ was adjusted to give a straight line, and the restricted-diffusion method described by Harned and French (1945) is used to determine the effective solute diffusion co-

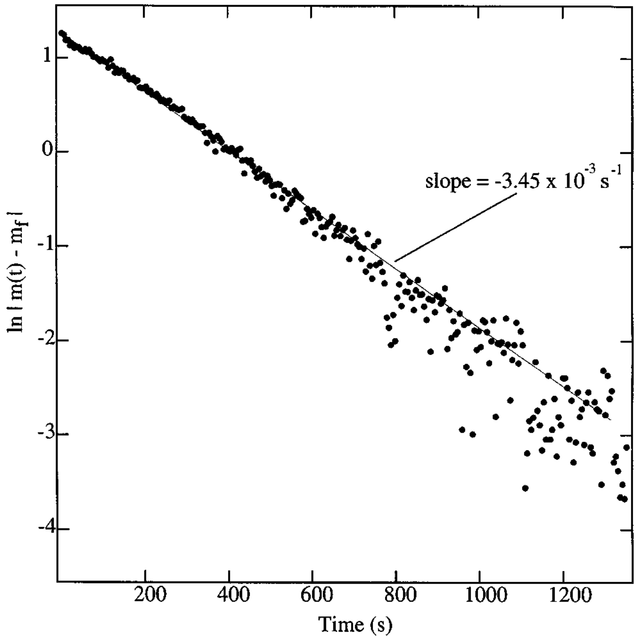

**Figure 10. Calculation of the effective diffusion coefficient from the uptake of methanol vapor at 60°C.**

The diffusion coefficient ($D = 1.01 \times 10^{-11}$ m²/s) is proportional to the slope of a line drawn through the data. The membrane's thickness is $168 \times 10^{-6}$ m. The final mass used for this calculation was $2.85 \times 10^{-4}$ kg, and the mass of the dry membrane was $2.51 \times 10^{-4}$ kg.

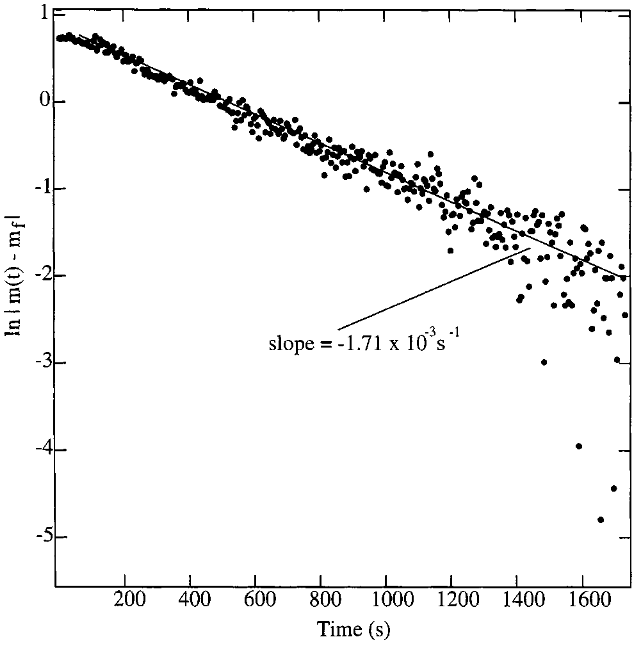

**Figure 11. Calculation of the effective diffusion coefficient from the uptake of water vapor at 60°C.**

The diffusion coefficient ($D = 4.87 \times 10^{-12}$ m²/s) is proportional to the slope of a line drawn through the data. The membrane's thickness is $165 \times 10^{-6}$ m. The final mass used for this calculation was $2.82 \times 10^{-4}$ kg, and the mass of the dry membrane was $2.51 \times 10^{-4}$ kg.

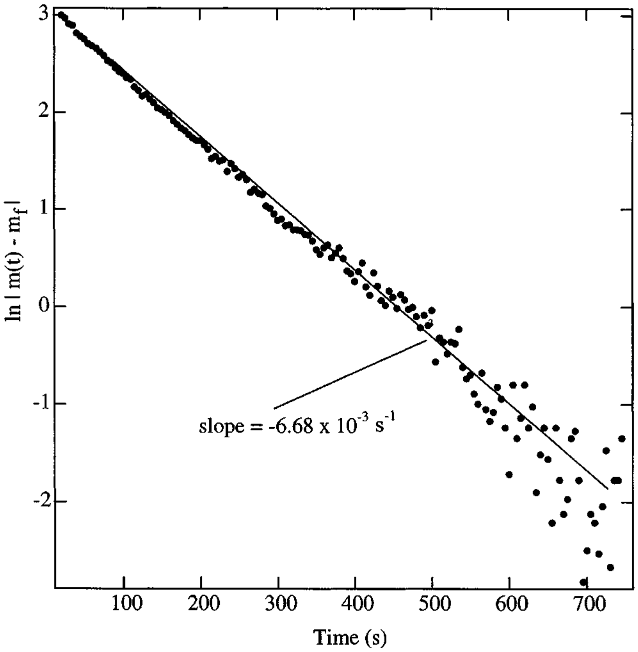

**Figure 12. Calculation of the effective diffusion coefficient from the uptake of the vapor from an equimolar liquid mixture of methanol and water at 60°C.**

The diffusion coefficient ($D = 1.87 \times 10^{-11}$ m²/s) is proportional to the slope of a line drawn through the data. The membrane's thickness is $164 \times 10^{-6}$ m. The final mass used for this calculation was $1.34 \times 10^{-4}$ kg, and the mass of the dry membrane was $2.51 \times 10^{-4}$ kg.

efficients shown in the figure captions. These values are $D = 1.01 \times 10^{-11}$ m²/s for uptake of methanol in a membrane previously soaked in water; $D = 4.87 \times 10^{-12}$ m²/s for uptake of water into the same membrane now saturated with methanol; and $D = 1.87 \times 10^{-11}$ m²/s for uptake of a mixed-solute vapor created from an equimolar liquid mixture of methanol and water. The first two results imply that methanol more readily diffuses in Nafion than does water. For comparison, we calculated the infinite dilution coefficient of methanol diffusing into water and water diffusing into methanol using the method described by Tyn and Calus (1975). These diffusion coefficients were calculated for 60°C and found to be on the order of $10^{-9}$ m²/s.

Previous work on the diffusion of water in Nafion has been carried out for uptake from both the liquid phase and the vapor phase. Zelsmann et al. (1990) measured the diffusion of water vapor as a function of water-vapor activity. Unfortunately, they give us neither the membrane's temperature nor its water composition. Without these data, we can only infer the order of magnitude of the diffusion coefficient. Their measurements yield results from $D = 5 \times 10^{-12}$ m²/s to $3 \times 10^{-11}$ m²/s. Fuller (1992) reports values from $D = 1.2 \times 10^{-10}$ m²/s to $1.8 \times 10^{-10}$ m²/s for uptake from the vapor phase. Fuller's experiments were controlled by fixing the activity of the vapor and allowing the membrane to equilibrate with the vapor phase. The results for uptake from the liquid phase are generally one order of magnitude larger. Yeo and Eisenberg (1977) give a value of $D = 2.3 \times 10^{-10}$ m²/s at 28°C. The val-

**Table 4a. Water Vapor Uptake in Nafion at 60°C***

| Total Pres. (Water Vapor) ($\times 10^2$ Pa) | Upper Spring Reading ($\times 10^{-3}$ m) | Lower Spring Reading ($\times 10^{-3}$ m) | Total Mass ($\times 10^{-6}$ kg) |
|---|---|---|---|
| 48 | 985.70 | 839.30 | 91.40 |
| 52 | 985.70 | 839.20 | 91.50 |
| 62 | 985.80 | 838.60 | 92.15 |
| 67 | 985.80 | 838.35 | 92.40 |
| 80 | 985.75 | 837.95 | 92.75 |
| 90 | 985.75 | 837.30 | 93.35 |
| 102 | 985.75 | 837.10 | 93.55 |
| 122 | 985.75 | 836.20 | 94.40 |
| 126 | 985.75 | 836.10 | 94.50 |
| 146 | 985.75 | 835.15 | 95.40 |
| 167 | 985.75 | 834.20 | 96.30 |
| 185 | 985.75 | 832.90 | 97.55 |
| 191 | 985.75 | 832.50 | 97.95 |
| 200 | 985.75 | 831.55 | 98.85 |

**Table 4b. Methanol Vapor Uptake at 60°C****

| | | | |
|---|---|---|---|
| 99 | 987.65 | 846.15 | 86.70 |
| 205 | 987.65 | 844.80 | 88.00 |
| 292 | 987.65 | 843.65 | 89.10 |
| 398 | 987.65 | 842.65 | 90.05 |
| 522 | 987.65 | 840.85 | 91.80 |
| 630 | 987.65 | 838.70 | 93.85 |
| 750 | 987.65 | 836.25 | 96.15 |
| 838 | 987.65 | 832.70 | 99.55 |

*Dry membrane mass, 87 ± 1 ($10^{-6}$ kg).
**Dry membrane mass, 82 ± 1 ($10^{-6}$ kg).

ues determined by Zawodzinski et al. (1993b) are obtained from vapor-phase uptake experiments, but are found by looking at length scales on the order of $10^{-6}$ m. Their intended measurement is the self-diffusion of water in the Nafion pore. They claim this value is related to the diffusion coefficient of water relative to the membrane by the factor $(d \ln a/d \ln C)$. Their values range from approximately $5\times10^{-11}$ m$^2$/s for $\lambda = 2$ to $5.5 \times 10^{-10}$ m$^2$/s for $\lambda = 14$.

## Conclusions

The solubility of a solute in Nafion increased in the presence of a second solute for uptake from the liquid phase. These uptake data were successfully fit with a thermodynamically consistent equation based on the Gibbs energy, thereby confirming that such a maximum is possible (see Figure 5). We are the first workers to treat the uptake of methanol and water in Nafion on a thermodynamic basis. A region of unconditional instability exists for methanol and water absorbed in Nafion. This region is enveloped by spinodal points, where the activities of two components go through extrema when the activity of the third component is held constant.

The measured uptake of pure methanol and pure water in Nafion at 60°C from the vapor phase showed discontinuities from what was measured for the liquid phase. This discontinuity is known in the literature as Schroeder's paradox. The uptake of water from the vapor phase at saturation conditions was $\lambda = 8.3$ vs. $\lambda = 22.0$ from the liquid. For methanol the values were $\lambda = 7.4$ and $\lambda = 21.5$, respectively.

The restricted diffusion method was used to determine the effective diffusion coefficients in Nafion at 60°C at three solute compositions. The effective diffusion coefficient is measured for diffusion from methanol vapor into a Nafion membrane containing water, water into a membrane containing methanol, and the vapor from an equimolar liquid mixture of methanol and water into a membrane containing water. The effective diffusion coefficients are found to be on the order of $10^{-11}$ m$^2$/s, comparable to diffusion coefficients noted in the literature for diffusion of a vapor into the membrane. The literature shows the diffusion coefficient to be an order of magnitude higher for diffusion from a liquid into Nafion.

## Acknowledgment

This work was supported by the Department of Defense/Army Research Office through the University of Minnesota.

## Literature Cited

Chapman, T. W., "The Transport Properties of Concentrated Electrolytic Solutions," PhD Thesis, Univ. of California, Berkeley (1967).

Fuller, T. F., "Solid-Polymer-Electrolyte Fuel Cells," PhD Thesis, Univ. of California, Berkeley (1992).

Harned, H. S., and D. M. French, "A Conductance Method for the Determination of Diffusion Coefficients of Electrolytes," *Ann. N.Y. Acad. Sci.*, **46**, 267 (1945).

Hauser, H., A. Heintz, B. Schmittecker, and R. N. Lichtenthaler, "Sorption Equilibria and Diffusion in Polymeric Membranes," *Fluid Phase Equilibria*, **51**, 369 (1989).

Heintz, A., and W. Stephan, "A Generalized Solution-Diffusion Model of the pervaporation Process Through Composite Membranes Part I. Prediction of Mixture Solubilities in the Dense Active Layer Using the UNIQUAC Model," *J. Memb. Sci.*, **89**, 143 (1994).

Hinatsu, J. T., M. Mizuhata, and H. Takenaka, "Water Uptake of Perfluorosulfonic Acid Membranes from Liquid Water and Water Vapor," *J. Electrochem. Soc.*, **141**, 1493 (1994).

Hirata, M., S. Ohe, and K. Nagahama, *Computer Aided Data Book of Vapor-Liquid Equilibria*, Kodansha Limited Elsevier Scientific Publishing Company, Tokyo (1975).

Nandan, D., H. Mohan, and R. M. Iyer, "Methanol and Water Uptake, Densities, Equivalent Volumes and Thicknesses of Several uni- and Divalent Ionic Perfluorosulphonate Exchange Membranes (Nafion-117) and Their Methanol-Water Fractionation Behaviour at 298 K," *J. Memb. Sci.*, **71**, 69 (1992).

Newman, J. S., "CLASS NOTES Chemical Engineering 141," Univ. of California, Berkeley (1985).

Schroeder, P., "Über Erstarrungs- und Quellungserscheinungen von Gelatine," *Z. Phys. Chem.*, **45**, 57 (1903).

Skou, E., P. Kauranen, and J. Hentschel, "Water and Methanol Uptake in Proton Conducting Nafion® Membranes," *Solid State Ionics*, **97**, 333 (1997).

Tyn, M. T., and W. F. Calus, "Diffusion Coefficients in Dilute Binary Liquid Mixtures," *J. Chem. Eng. Data*, **20**, 106 (1975).

Yeo, S. C., and A. Eisenberg, "Physical Properties and Supermolecular Structure of Perfluorinated Ion-Containing (Nafion) Polymers," *J. Appl. Poly. Sci.*, **21**, 875 (1977).

Zawodzinski, T. A., Jr., Derouin, S. Radzinski, R. J. Sherman, V. T. Smith, T. E. Springer, and S. Gottesfeld, "Water Uptake by and Transport Through Nafion 117 Membranes," *J. Electrochem. Soc.*, **140**, 1041 (1993a).

Zawodzinksi, T. A., Jr., T. E. Springer, J. Davey, J. Valerio, S. Gottesfeld, C. Lopex, and R. Jestel, "A Comparative Study of Water Update By and Transport Through Ionomeric Fuel Cell Membranes," *J. Electrochem. Soc.*, **140**, 1981 (1993b).

Zawodzinski, T. A., Jr., M. Neeman, L. O. Sillerud, and S. Gottesfeld, "Determination of Water Diffusion Coefficients in Perfluorosulfonate Inomeric Membranes," *J. Phys. Chem.*, **25**, 6040 (1991).

Zelsmann, H. R., and M. Pineri, "Water Self-Diffusion Coefficient Determination in an Ion Exchange Membrane by Optical Measurement," *J. Appl. Poly. Sci.*, **41**, 1673 (1990).

*Manuscript received Apr. 29, 1999, and revision received Apr. 14, 2000.*